Measurement 189 (2022) 110495

Contents lists available at ScienceDirect

Measurement

journal homepage: www.elsevier.com/locate/measurement

Diamond protection for reusable ZnO coated fiber-optic measurement head in optoelectrochemical investigation of bisphenol A

Małgorzata Szczerska [a,*], Monika Kosowska [b,*], Paulina Listewnik [a], Michał Rycewicz [a], Mikhael Bechelany [c], Yafit Fleger [d], Dror Fixler [d,e], Paweł Jakóbczyk [a]

[a] Department of Metrology and Optoelectronics, Faculty of Electronics, Telecommunications and Informatics, Gdańsk University of Technology, 11/12 Narutowicza Street, Gdańsk, Poland
[b] Faculty of Telecommunications, Computer Science and Electrical Engineering, Bydgoszcz University of Science and Technology, Al. prof. S. Kaliskiego 7, 85-796 Bydgoszcz, Poland
[c] Institut Europeén Des Membranes, IEM, UMR 5635, Univ of Montpellier, CNRS, ENSCM, 34095 Montpellier Cedex 5, France
[d] Institute for Nanotechnology and Advanced Materials, Bar-Ilan University, Ramat-Gan 52900, Israel
[e] Faculty of Engineering, Bar-Ilan University, Ramat-Gan 52900, Israel

ARTICLE INFO

Keywords:
Nanocrystalline diamond sheet
Zinc oxide
ZnO
Fiber-optic sensors
Measurement head protection
bisphenol A
Optoelectrochemical system

ABSTRACT

Due to the global problem with plastic contaminating the environment, with bisphenol A (BPA) being one of the highest demand, effective monitoring and purification of the pollutants are required. The electrochemical methods constitute a good solution but, due to polymerization of electrochemical oxidation bisphenol A products and their adsorption to the surfaces, measurement head elements are clogged by the formed film. In this research, we propose a nanocrystalline diamond sheet protection for securing elements in direct contact with bisphenol A during electrochemical processes. The solution was presented on the example of a zinc oxide (ZnO) coating deposited on a fiber-optic end-face by Atomic Layer Deposition. Series of optical and electrochemical measurements were performed in a dedicated hybrid setup. The results show that ZnO can be modified during the electrochemistry leading to the drastic change of its properties. Such degradation did not show in case of nanocrystalline diamond sheet-protected sample proving the solution's effectiveness, giving a possibility of re-using the measurement element and prolonging its lifespan.

1. Introduction

Nowadays, the role of plastic is enormous as it is extensively used in many branches of industry due to the ease of processing and low acquisition costs compared to other materials. However, the price of its overuse is a serious ecological problem, as most plastics are not biodegradable or decompose very slowly. One of the most produced chemicals in the world is bisphenol A: global usage reached around 7.7 million metric tons in 2015 and it is expected to increase up to 10.6 tons by 2022 [1]. Bisphenol A is a synthetic compound that is a precursor in production of plastics that are widely used for fabrication of e.g. water bottles and food storage containers. In the recent years, many researchers focused on the investigation of bisphenol A and its impact on environment translating to humans and animals [2-4]. Studies on bisphenol A show a potential risk on health e.g. it can interfere with hormone systems [5-8].

As bisphenol A occurrence in the environment is a result of human activities, the main sources of its release are industry production and processing, wastewater treatment plant discharges, and degradation of polymers [6,9,10]. Hence, several methods answering the need for bisphenol A effective monitoring and water purification were proposed [11], including biological [12-14], photochemical [15], physical adsorption [9,16,17] and electrochemical methods [18-20]. Among those, the electrochemical techniques are distinguished by the smallest secondary pollution as no additional reactive chemicals are required and the treatment activity is independent from the substance toxicity like in case of biological methods [21]. However, despite many solutions, bisphenol A remains a challenging substance to be investigated. Due to

Abbreviations: ALD, Atomic Layer Deposition; BDD, Boron Doped Diamond; BPA, Bisphenol A; CA, Chronoamperometry; CV, Cyclic Voltammetry; CVD, Chemical Vapor Deposition; EC, Electrochemistry; NDS, Nanocrystalline Diamond Sheet; ZnO, Zinc Oxide.

* Corresponding authors.
E-mail addresses: malszcze@pg.edu.pl (M. Szczerska), monika.kosowska@pbs.edu.pl (M. Kosowska).

https://doi.org/10.1016/j.measurement.2021.110495
Received 1 September 2021; Received in revised form 17 November 2021; Accepted 18 November 2021
Available online 23 November 2021

polymerization, some of its electrochemical oxidation products adsorb to the surface of the electrodes making them clogged and decreasing surface redox performance [22]. As assessed through cyclic voltammetry, the electrooxidation of bisphenol A (BPA) is an irreversible process; furthermore, if repetitive cycling is carried out, the oxidation signal disappears due to the possible formation of a polymeric film on the surface of measurement setup elements.

In this research, we show a hybrid system applying optical and electrochemical methods for performing and monitoring the electrochemical (EC) processes. The setup allowed investigation of the bisphenol A impact on the measurement head components (on an example of a ZnO coated optical fiber) as well as a way to secure the head against clogging.

A fiber-optic sensor was chosen as it assures high sensitivity and wide dynamic range of measurements, as well as current-free operation of the measurement head which uses only light [23]. The dielectricity allows for coupling it with other methods due to the lack of operation interference. Fiber-optic sensors can be used to determine values of many quantities e.g. temperature [24], refractive index [25], pH [26], pressure [27], displacement [28], among others [29,30]. They enable measurements in places hard to reach and in difficult working conditions. On the other hand, zinc oxide (ZnO) is an interesting material which usage can benefit many optoelectronic solutions. It is an n-type semiconductor characterized by a wide band gap (3.36 eV), refractive index of 1.9–2, and biocompatibility [31]. It found its application in sensors and other optoelectronics devices [32-34].

The use of ZnO in fiber-optic sensors results in broadening the measurement range and improves the sensitivity while comparing to solutions without the coating. Furthermore, its deposition allows measurements of media characterized by refractive index values close to the optical core. Properties of ZnO can be tailored during the deposition process, altering e.g. its thickness or refractive index. Hence, ZnO coating was applied to the measurement head in our optical setup without and with nanocrystalline diamond sheet over its surface to protect it from bisphenol A impact. Reasoning behind the application of a synthetic diamond structure lies in its extraordinary properties starting with resistance to biological, chemical and mechanical damages, high hardness, chemical stability and biocompatibility. Moreover, when undoped, it is transparent in a wide wavelength range, from ultraviolet to infrared [hidden].

In this research we propose a nanocrystalline diamond sheet as a protection of the measurement head during electrochemical processes. We used a hybrid system coupling a Fabry-Perot interferometer with a standard 3-electrode electrochemical cell. In such configuration the boron-doped diamond film played a dual role of a mirror and a working electrode. The optical fiber end-face served as a measurement head and was covered with a ZnO layer deposited by Atomic layer Deposition (ALD). We performed electrochemical processes of bisphenol A with unprotected ZnO coated fiber and ZnO coated fiber using nanocrystalline diamond sheet (NDS) to assess its ability to protect elements surfaces. The goal of this research is to prove that the nanocrystalline diamond sheet can serve as efficient protection of the exposed elements of the measurement head in contact with bisphenol A. The demonstration will be carried out on example of ZnO state changes caused by BPA.

2. Experimental details

2.1. Optoelectrochemical system

The optoelectrochemical system for simultaneous interferometric and electrochemical measurements was constructed from a Fabry-Perot interferometer and 3-electrode electrochemical setup. Both parts were combined by a boron-doped diamond film playing a dual role of a mirror and a working electrode.

The Fabry-Perot cavity was formed between the two boundaries: fiber end-face/ investigated medium and investigated medium/boron-doped diamond film. The incident light from the light source (SLD-1550–13-, FiberLabs Inc., Japan), was guided by the fiber and partially reflected on the first and the second interface as shown in Fig. 1. The beams interfered with each other giving a signal dependent on their optical path difference influenced by e.g. changes in refractive index of the medium inside the cavity or the cavity length itself. The measurement signal was recorded by the optical spectrum analyzer (Ando AQ6319, Yokogawa, Japan).

The electrochemical measurements were investigated by cyclic voltammetry (CV), and chronoamperometry (CA). The EC measurement system consists of the working electrode (boron doped diamond, BDD), having an area of 0.2 cm^2, the counter electrode is a platinum wire and the reference electrode is an AgCl-coated Ag wire. The measurement of electrochemical working electrode properties was carried out in 1 M KNO_3/1mM $Fe(CN)_6^{3-/4-}$ solution as the electrolyte, at scan rate 100 mV/s. Electrochemical oxidation (CA) and characterization of bisphenol A (CV) was taken in 200 mg/L bisphenol A solution in 0.5 M Na_2SO_4 using a potentiostat–galvanostat (VMP-300, Bio-Logic, France) driven by EC-Lab software.

This hybrid setup is presented in Fig. 2, its detailed description can be found elsewhere [35].

2.2. Chemicals

The Sodium sulfate (ACS reagent, purity ≥ 99%, Aldrich), potassium hexacyanoferrate(II) and potassium hexacyanoferrate (III) (Pure p. a., Chempur), aqueous solutions were prepared using demineralised water. Bisphenol A (purity: 97%) was attained from Aldrich. The Potassium nitrate (pure p.a.) and sulfuric acid (purity ≥ 95%,) were purchased from Chempur. Diethylzinc (min. 95%) was purchased from Strem Chemicals. The synthesis gases: methane, hydrogen, argon and diborane were collected from Linde and were of the highest purity class.

All reagents were used as received from the suppliers.

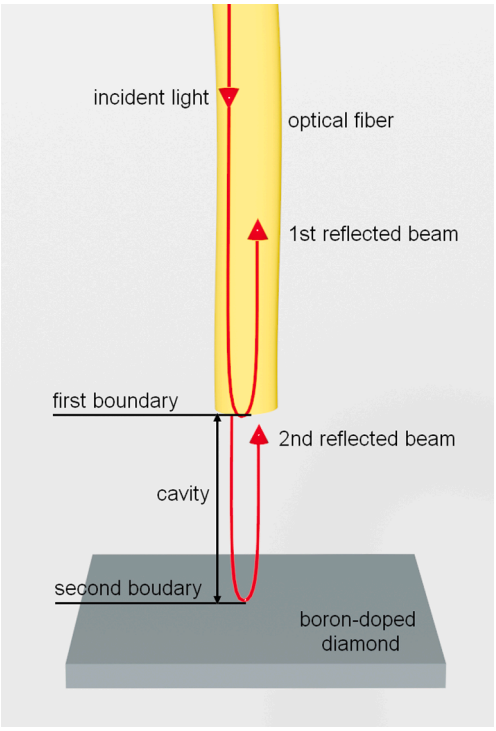

Fig. 1. Principle of operation. Fiber-optic realization of a Fabry-Perot interferometer where boron-doped diamond plays a role of a mirror.

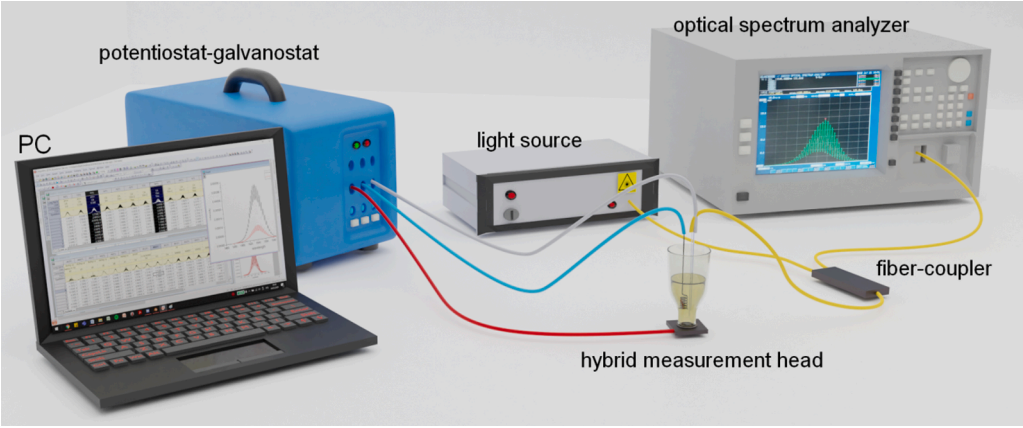

Fig. 2. Measurement setup. Optoelectrochemical system coupling 3-electrode electrochemical cell with a Fabry-Perot interferometer.

2.3. ZnO layer deposition

A home-made ALD set-up was used for depositing of ZnO thin layers of 100 nm on the surface of the optical fibers. The detailed descriptions of the ZnO layer deposition are reported elsewhere [36,37].

2.4. Diamond structures

Diamond layers were grown in a Microwave Plasma Enhanced Chemical Vapor Deposition reactor with a frequency of 2.45 GHz (SEKI Technotron AX5400S, Japan) on mirror-polished tantalum foils (0.4 mm thick) and p-type silicon wafers with (100) orientation. Before the growth, the substrates were cleaned by sonication in acetone and 2-propanol for 10 min. After the cleaning step they were seeded with water suspension consisting of diamond particles. The crystallite size was 4–7 nm.

Due to different substrates, diamond layers were grown in two separate processes.

2.4.1. Boron-doped diamond growth

To grow diamonds on silicon, we used 1300 W of microwave power. The temperature of the graphite stage, on which samples were laying, was set to 700 °C. Samples were doped using diborane. [B]/[C] ratio was 10 000 ppm. The pressure inside the chamber was 50 Torr, while the total flow rate – 300 sccm (CH_4:H_2 ratio was 1:100). After 12 h of process, the substrates were placed in boiling H_2SO_4 and KNO_3 solution (2:1 wt ratio) for 30 min. Next, the boron-doped diamond was ultrasonicated in isopropyl alcohol and deionized water for 10 min. In the end, the electrodes were hydrogenated in the Microwave Plasma Enhanced CVD reactor (1100 W, 50 Torr, 15 min).

2.4.2. Diamond sheet growth

In contrast to boron-doped diamond on silicon, the microwave power and temperature of the graphite stage were 1.1 kW and 500 °C, respectively. A detailed description of the diamond sheet growth can be found in [35]. Table 1 presents comparison of the deposition parameters to obtain different diamond structures.

The most crucial part of the nanocrystalline diamond assessment before using it as a protective layer was to investigate its morphology. Scanning Electron Microscopy (SEM) images were taken with an Environmental Scanning Electron Microscope (E-SEM, Quanta FEG 250, FEI, Hillsboro, Oregon, USA) while Focused-Ion Beam (FIB) system (Helios UC5, Thermo-Fisher, Waltham, Massachusetts, USA) was used for cross-section imaging and are presented in Fig. 3.

As can be seen from the obtained images, the diamond sheet is formed from uniformly distributed crystals. No discontinuities, holes or cracks are present, assuring a full coverage of the target surface. In order to measure the thickness of the nanocrystalline diamond sheet, cross-section cuts were done using FIB with voltage-current of 5 kV and 0.8nA. The measured thickness of the sheet is equal to 1.558 μm. Thanks to appropriate selection of deposition parameters we achieved a structure with low adhesion to the substrate. As a result, introduction of external stress causes the detachment of the diamond structure from tantalum substrate. Such realized free-standing flake can be then transferred onto the desired surface.

3. Results and discussion

In order to investigate the effectiveness of the nanocrystalline diamond sheet on protection of a ZnO layer, we performed series of measurements using optoelectrochemical setup and a Fabry-Perot interferometer with a silver mirror. First, the distance measurements were performed in the range of 0–1000 μm for a measurement head with deposited ZnO. Then, the electrochemical processes were carried out with the measurement head immersed in the electrochemical cell filled with solution. During EC, a boron-doped diamond film was used as a dual-role element acting simultaneously as a working electrode and a reflective layer, as shown in Fig. 4.

The last step was to perform the distance measurements again under the same settings to evaluate potential changes in ZnO condition. This procedure was conducted twice: for a fiber with a bare ZnO layer and for a ZnO protected with a nanocrystalline diamond sheet during the electrochemical processes. The flowchart of the experiment is shown in the Fig. 5.

Electrochemical part of the measurements included 5 steps: cyclic voltammetry (CV) with ferrycyanides to assess if the boron-doped diamond operates properly as a working electrode, CV with bisphenol A solution, chronoamperometry (CA) in four 5-minute series, and again CVs: with bisphenol A and next in ferrycyanides. During all those steps the optical fiber with ZnO layer was immersed in the liquid to optically

Table 1
Deposition parameters for diamond structures.

structure	deposition time	microwave power	temperature of the stage	pressure	total flow rate	CH_4:H_2 ratio	substrate
boron-doped diamond	12 h	1300 W	700 °C	50 Torr	300 sccm	1:100	silicon wafer
nanocrystalline diamond sheet	3 h	1100 W	500 °C	50 Torr	300 sccm	1:100	tantalum sheet

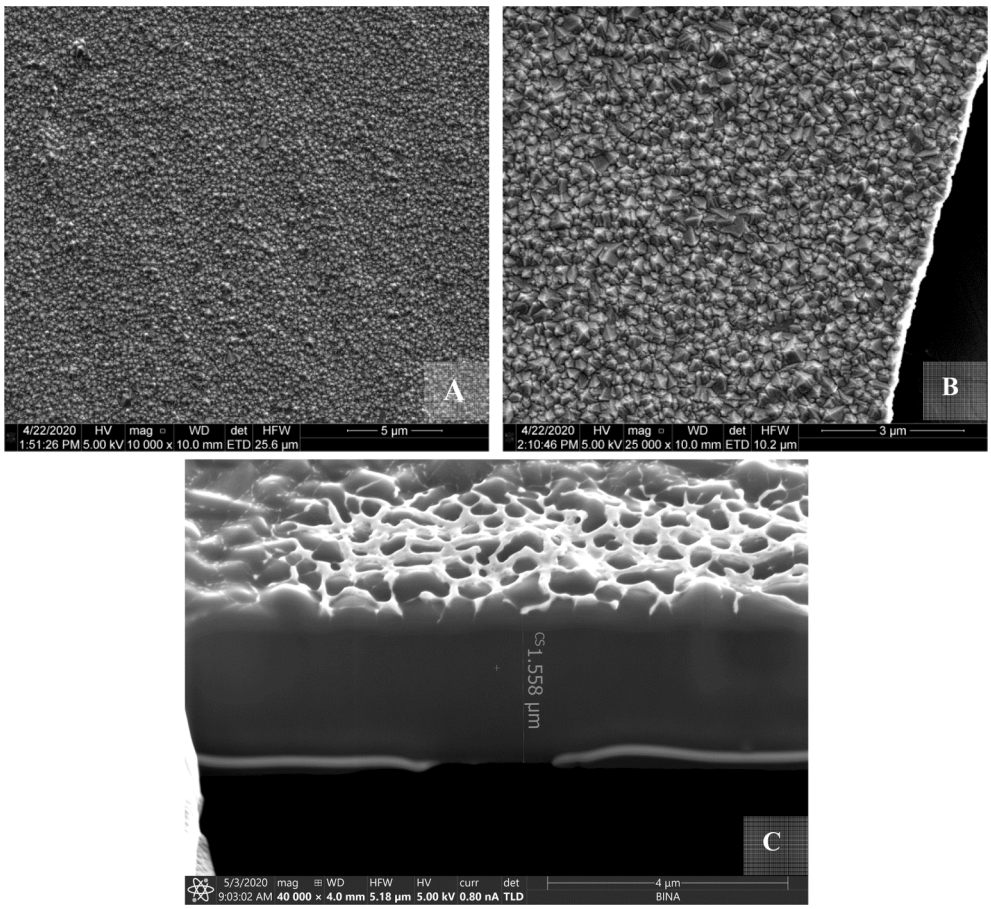

Fig. 3. SEM images of a nanocrystalline diamond sheet. (A) magnification 10,000x (B) magnification 25,000x with visible structure edge (C) cross-section with thickness measurement. The images show uniform distribution of crystallites forming the sheet with no cracks or defects in the structure. Note that the sheet area is large enough to cover a fiber end-face (8 µm fiber-core diameter).

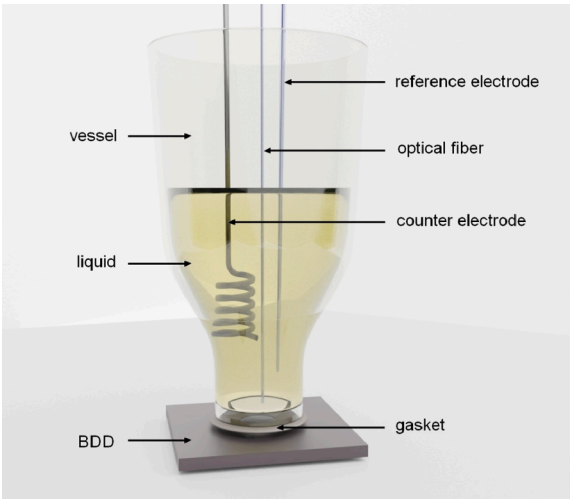

Fig. 4. Optoelectrochemical measurement head scheme. The boron-doped diamond works as a working electrode and a mirror. The fiber end-face is coated with a 100 nm ZnO layer. The EC measurements were performed twice: for a fiber with bare ZnO and with application of NDS over it.

monitor changes of investigated processes. Then, we repeated all steps for optical fiber with ZnO layer covered with NDS.

The electrooxidation process of organic compounds such as bisphenol A on BDD electrodes is one of the ways of removing this compound from wastewater, where its concentration is the highest. Several research groups investigate the BDD electrodes as a solution [38-40], hence in our investigation we decided to use such a model system.

However, as mentioned in the introduction, the compounds of electrochemical oxidation of bisphenol A can cover the electrode surface. As a result, the electrode is blocked and unable to be used again in further experiments. This phenomenon is shown in the Fig. 6. A cyclic voltammetry with ferrycyanides was performed to ensure a proper operation of the BDD as a working electrode (black curve). The standard voltammogram was obtained with clear oxidation (point A: E = 0.2401 V, I = 0.0174 mA) and reduction (point B: E = 0.1243 V, I = -0.0161 mA) peaks. As the graph is in agreement with theoretical shape of the curve for chemical reactions which rates are dependent on diffusion of the analyte to and from the planar working electrode, we conclude that the BDD operates properly [41].

Clear oxidation and reduction peaks were obtained and a shape of the curve is in agreement with theory. Next, series of EC processes was carried out: CV with bisphenol A, 4 series of 5 min CA for the oxidation of bisphenol A, and again CV with bisphenol A to assess the effectiveness of the bisphenol A oxidation process. After the ECs, a verification of the electrode usability was needed. Hence, we performed another cyclic voltammetry process with ferrocyanides with the same settings as prior to EC with bisphenol A. As expected, the recorded curve was significantly different from the theoretical curve indicating a properly functioning working electrode. No oxidation and reduction peaks were registered this time proving that the electrode was clogged (red curve).

The clogging process was additionally observed by the analysis of the optical spectra recorded during the EC investigation. Representative

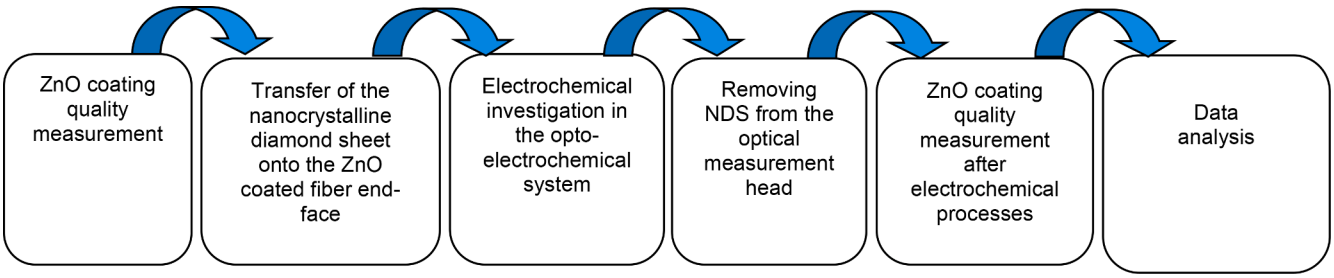

Fig. 5. Flowchart of the experimental process.

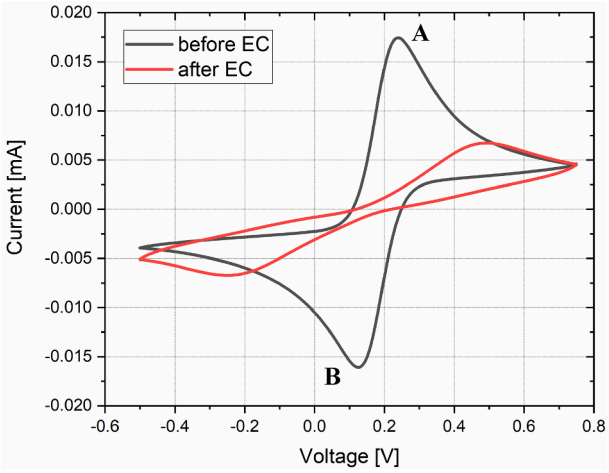

Fig. 6. Cyclic voltammograms. The comparison of the curves before and after EC reactions including bisphenol A. At the beginning the electrode worked properly, assuring visible oxidation (point A) and reduction (point B) peaks. After the EC series, bisphenol A compounds clogged the electrode and, as a result, it cannot be reused.

signals taken while the optical measurement head was immersed in the liquid while chronoamperometry process was running is shown in Fig. 7.

The spectra are altered along with the progressing EC process: the signal intensity and the spectrum modulation change. The quality of the signal can be assessed by the value of signal visibility, also called contrast. The higher its value, the better signal quality. The visibility of the signal can be expressed as [42]:

$$V = \frac{P_{max} - P_{min}}{P_{max} + P_{min}}$$

where V is visibility, P_{max} and P_{min} are the maximum and minimum signal values (Fig. 8), respectively.

Similarly to the BDD, an optical measurement head can be affected by EC processes leading to its damage. To avoid it, we propose a nanocrystalline diamond sheet (NDS) as a protective coating.

The measurements assessing impact of the NDS protection were taken on silver mirror, with air inside the Fabry-Perot cavity set to 100 μm (Fig. 9), in order to keep a ZnO layer condition as the only variable. For the comparison, the measurements were performed for the newly ZnO coated fiber (the reference) and two fibers after the whole EC procedure: without and with NDS protection during EC.

Representative signals acquired for a ZnO measurement head before and after EC as well as for a measurement head with NDS-protected ZnO during EC are shown in Fig. 10.

The measurements taken before and after the electrochemical processes show that unprotected ZnO coated fiber head is prone to bisphenol A impact which drastically changes the spectrum modulation, meaning that such measurement head cannot be used again due to different coating properties. In case of nanocrystalline diamond sheet protected sample, we achieved the same signal modulation as shown in Fig. 11.

The direct comparison of the acquired spectra proves that the application of a nanocrystalline diamond sheet is beneficial toward prolonging the lifespan of system elements. The reusability achieved this way greatly reduces the cost of the measurements since another process of a new sample deposition is not required as the material properties are

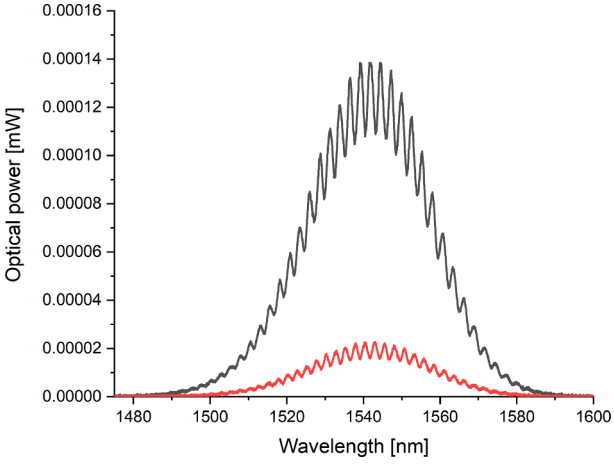

Fig. 7. Representative spectra recorded during the chronoamperometry process. Black line – spectrum recorded while the measurement head was immersed in the liquid (reference measurement), red line – spectrum acquired during electrochemical process. The change of the optical signal properties due to progressing clogging effect can be observed.

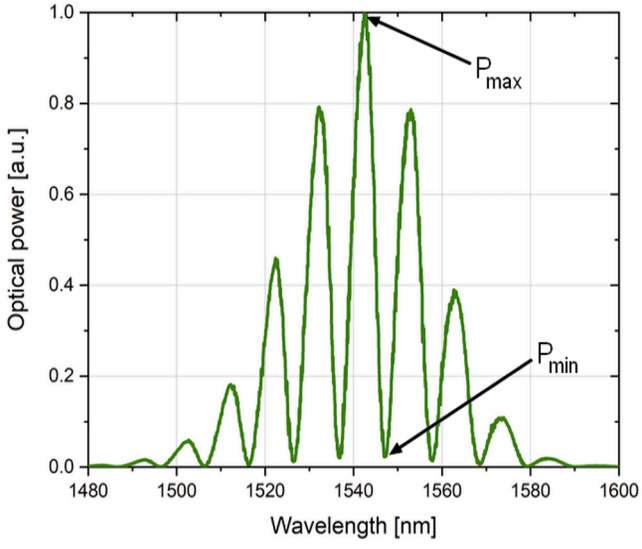

Fig. 8. Representative optical spectrum. Maximum and minimum signal values (P_{max}, P_{min}, respectively) for visibility calculation are marked'

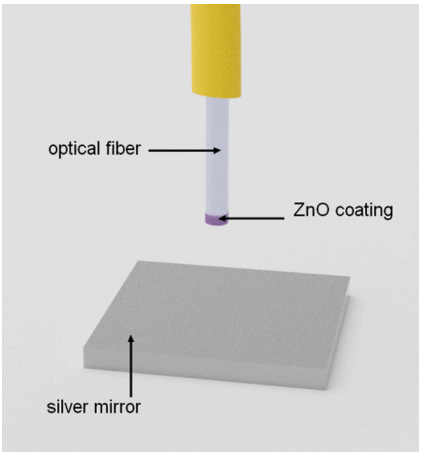

Fig. 9. Measurement head for ZnO coating state assessment.

maintained.

The optical spectra clearly show that the parameters of the ZnO layer have changed as a result of its exposure to liquids and electrochemical reactions. On the other hand, the ZnO layer that was protected by nanocrystalline diamond sheet keeps the same signal modulation. As can be seen from the Table 2, the spectral characteristics are nearly the same in case of starting ZnO state and after its usage with NDS during EC processes. Slight differences can be attributed to the possible misalignment of the head setting during its assembly in a micromechanical system. On the other hand, the unprotected ZnO shows drastically different spectral parameters, starting with a central maximum shift, different signal modulation revealed in smaller spectral separation of fringes and greater number of maxima in the investigated wavelength range, ending with significantly increased absorption (from 0.02 to 0.12) and large visibility drop (from 0.96 to 0.78). The experiment proves that the nanocrystalline diamond sheet is a promising structure in terms of interface protection. It allows performing measurements as normal, giving expected results, while protecting the targeted surface from chemical damage.

4. Conclusions

In this paper we propose a nanocrystalline diamond sheet for protection of a ZnO coated fiber end-face while performing electrochemical investigation of bisphenol A. The research outcome of this study shows that bisphenol A impacts the properties of measurement elements in direct contact with it: the working electrode and a ZnO layer making them impossible to reuse. On the other hand, the results of this investigation proved that the NDS protection applied for the ZnO allowed to maintain its properties as indicated by the same spectrum modulation while comparing signals registered before and after the EC. With our hybrid optoelectrochemical setup we are able to continuously monitor the state of the sample, and after the measurements easily extract the optical measurement head to individually assess the quality of the ZnO layer.

The research contribution of this study lies in a method of protecting the exposed elements of measurement heads in direct contact with bisphenol A. Its effectiveness was presented on example of ZnO: it was demonstrated that it can be modified by BPA during the EC measurements leading to the drastic change of its properties, which can be prevented by protecting its surface with NDS. This approach gives us possibility of re-using the same measurement head and prolonging its

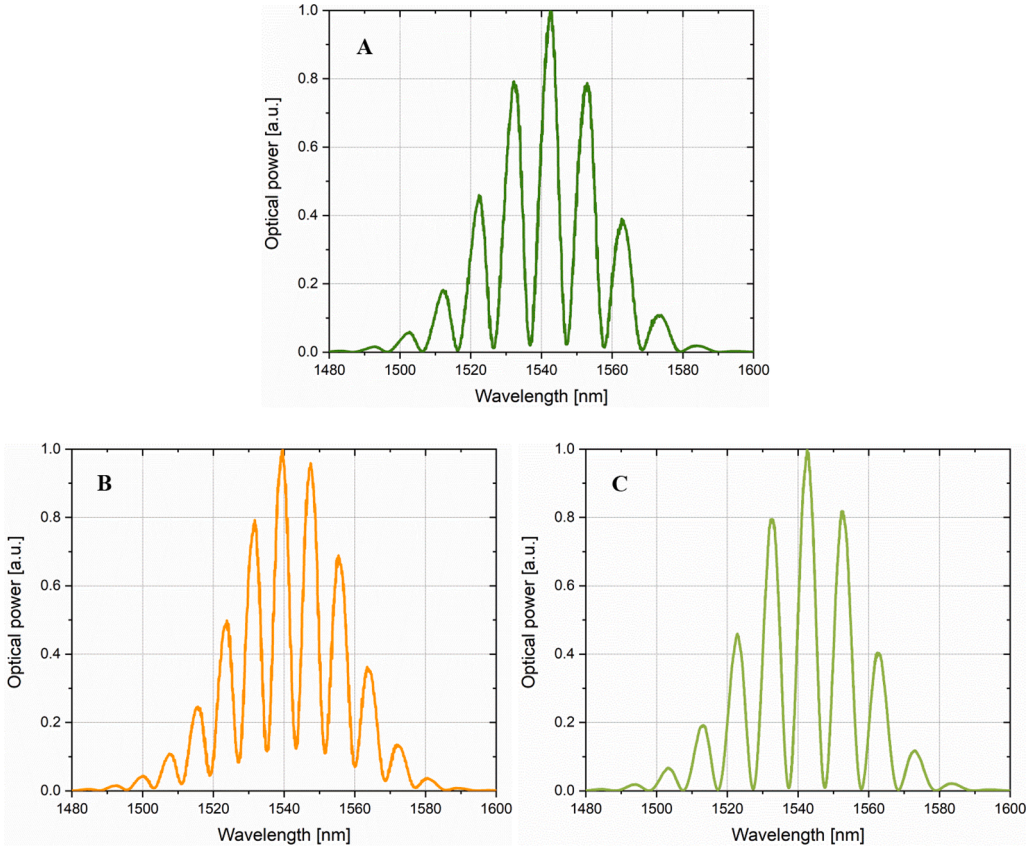

Fig. 10. Spectra comparing ZnO state before and after EC. (A) Measurement head with ZnO before EC (B) Measurement head with bare ZnO during EC (C) Measurement head with ZnO and NDS during EC, with NDS removed afterwards. A drastic change in signal can be observed for the uncovered ZnO during EC in comparison to the sample covered with NDS. Different signal modulation in (B) indicates degeneration of the initial ZnO parameters which was avoided in case of (C).

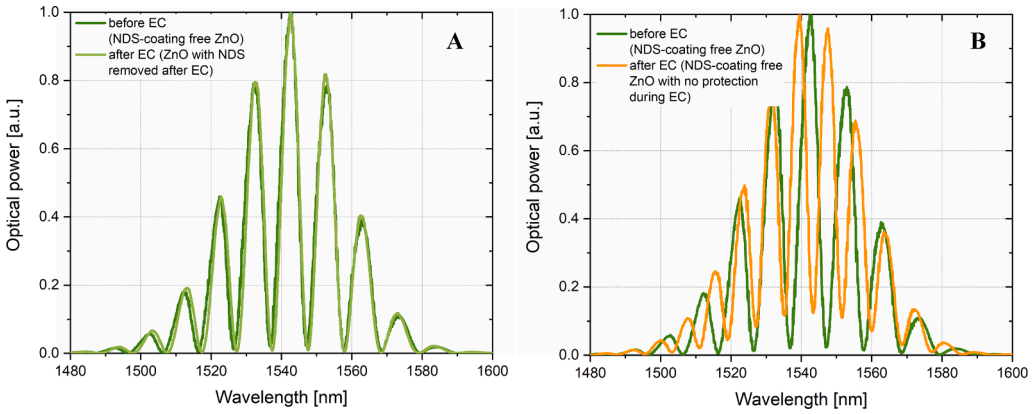

Fig. 11. Direct comparison of spectra for investigated measurement head configurations. (A) The NDS-protected ZnO coating maintained its properties which is proved by the same spectral response before and after EC. (B) Visible ZnO degradation occurred as indicated by a signal change.

Table 2
Comparison of spectra properties. Note a significant change in parameters for an unprotected ZnO fiber.

Parameter	before EC	after EC with NDS protection	after EC with no protection
Central maximum [nm]	1542.46	1542.56	1539.64
Spectral separation [nm]	10.24	9.94	7.92
Number of maxima in the range of 1500 ÷ 1580 nm	7.94	8.03	10.00
Absorption	0.02	0.01	0.12
Visibility	0.96	0.98	0.78

lifespan, which can be beneficiary for further development of solutions dedicated to removal of the bisphenol A from the environment as it is recognized as potential risk for human health. Application of nanocrystalline diamond sheets for securing elements and films from chemically aggressive substances will have impact on opening new perspectives for devices development. Future research will aim at optimizing the transfer technique of the NDS onto different surfaces and examine its securing abilities against other chemicals, potentially dangerous for measurement head elements.

CRediT authorship contribution statement

Małgorzata Szczerska: Conceptualization, Methodology, Supervision, Writing – review & editing. **Monika Kosowska:** Conceptualization, Methodology, Investigation, Visualization, Writing – original draft. **Paulina Listewnik:** Conceptualization, Methodology. **Michał Rycewicz:** Writing – original draft. **Mikhael Bechelany:** Writing – original draft. **Yafit Fleger:** Investigation, Visualization. **Dror Fixler:** Supervision, Writing – review & editing. **Paweł Jakóbczyk:** Conceptualization, Methodology, Investigation, Writing – original draft.

Declaration of Competing Interest

The authors declare that they have no known competing financial interests or personal relationships that could have appeared to influence the work reported in this paper.

Acknowledgements

Financial support of these studies from Gdańsk University of Technology by the 11/2020/IDUB/I.3/CC grant under the Curium Combating Coronavirus - EIRU program is gratefully acknowledged. The research was supported by Polish National Agency for Academic Exchange – NAWA under bilateral exchange of scientists between France and Poland PHC Polonium (PPN/BFR/2019/1/00005), and the DS Programs of Faculty of Electronics, Telecommunications and Informatics of the Gdańsk University of Technology. This work has been also supported by the DS funds of the Faculty of Telecommunications, Computer Science and Electrical Engineering, Bydgoszcz University of Science and Technology. Monika Kosowska acknowledges support from Polish National Agency for Academic Exchange under the Iwanowska Programme (PPN/IWA/2018/1/00058/U/0001). Paweł Jakóbczyk gratefully acknowledges financial support from The National Centre for Research and Development NOR/POLNOR/i-CLARE/0038/2019. Michał Rycewicz acknowledges the financial support of the National Agency for Academic Exchange under the Iwanowska Programme (PPN/IWA/2019/1/00091/U/00001) and TU Delft (Faculty of Mechanical, Maritime and Materials Engineering) for sharing the equipment.

References

[1] H.-J. Lehmler, B. Liu, M. Gadogbe, W. Bao, Exposure to Bisphenol A, Bisphenol F, and Bisphenol S in U.S. Adults and Children: The National Health and Nutrition Examination Survey 2013–2014, ACS Omega. 3 (2018) 6523–6532, https://doi.org/10.1021/acsomega.8b00824.
[2] Cyrene J. Catenza, Amna Farooq, Noor S. Shubear, Kingsley K. Donkor, Chemosphere 268 (2021) 129273, https://doi.org/10.1016/j.chemosphere.2020.129273.
[3] Zineb Kadri, Issam Mechnou, Souad Zyade, Mater. Today:. Proc. 45 (2021) 7584–7587, https://doi.org/10.1016/j.matpr.2021.02.581.
[4] Radia Bousoumah, Veruscka Leso, Ivo Iavicoli, Pasi Huuskonen, Susana Viegas, Simo P. Porras, Tiina Santonen, Nadine Frery, Alain Robert, Sophie Ndaw, Sci. Total Environ. 783 (2021) 146905, https://doi.org/10.1016/j.scitotenv.2021.146905.
[5] D. Nesan, K.M. Feighan, M.C. Antle, D.M. Kurrasch, Gestational low-dose BPA exposure impacts suprachiasmatic nucleus neurogenesis and circadian activity with transgenerational effects, Science, Advances. 7 (2021) eabd1159, https://doi.org/10.1126/sciadv.abd1159.
[6] Susana Almeida, António Raposo, Maira Almeida-González, Conrado Carrascosa, Bisphenol A: Food Exposure and Impact on Human Health, Compr. Rev. Food Sci. Food Saf. 17 (6) (2018) 1503–1517, https://doi.org/10.1111/crf3.2018.17.issue-610.1111/1541-4337.12388.
[7] Jae Kwan Kim, Adnan Khan, Seongha Cho, Jinhyuk Na, Yeseung Lee, Geul Bang, Wook-Joon Yu, Ji-Seong Jeong, Sun Ha Jee, Youngja H. Park, Effect of developmental exposure to bisphenol A on steroid hormone and vitamin D3 metabolism, Chemosphere 237 (2019) 124469, https://doi.org/10.1016/j.chemosphere.2019.124469.
[8] X. Zhang, H. Chang, S. Wiseman, Y. He, E. Higley, P. Jones, C.K.C. Wong, A. Al-Khedhairy, J.P. Giesy, M. Hecker, Bisphenol A Disrupts Steroidogenesis in Human H295R Cells, Toxicol. Sci. 121 (2011) 320–327, https://doi.org/10.1093/toxsci/kfr061.
[9] M.S. Muhamad, M.R. Salim, W.J. Lau, Z. Yusop, T. Hadibarata, The Removal of Bisphenol A in Water Treatment Plant Using Ultrafiltration Membrane System, Water Air Soil Pollut. 227 (2016) 250, https://doi.org/10.1007/s11270-016-2951-7.
[10] P. Mercea, Physicochemical processes involved in migration of bisphenol A from polycarbonate, J. Appl. Polym. Sci. 112 (2) (2009) 579–593, https://doi.org/10.1002/app.v112:210.1002/app.29421.
[11] H. Wang, Z. Liu, J. Zhang, R. Huang, H. Yin, Z. Dang, P. Wu, Y. Liu, Insights into removal mechanisms of bisphenol A and its analogues in municipal wastewater treatment plants, Sci. Total Environ. 692 (2019) 107–116, https://doi.org/10.1016/j.scitotenv.2019.07.134.

[12] Magdalena Zielińska, Irena Wojnowska-Baryła, Agnieszka Cydzik-Kwiatkowska, in: Bisphenol A Removal from Water and Wastewater, Springer International Publishing, Cham, 2019, pp. 61–78, https://doi.org/10.1007/978-3-319-92361-1_4.
[13] Magdalena Noszczyńska, Michalina Chodór, Łukasz Jałowiecki, Zofia Piotrowska-Seget, A comprehensive study on bisphenol A degradation by newly isolated strains Acinetobacter sp. K1MN and Pseudomonas sp. BG12, Biodegradation 32 (1) (2021) 1–15, https://doi.org/10.1007/s10532-020-09919-6.
[14] Robert Frankowski, Agnieszka Zgoła-Grześkowiak, Wojciech Smułek, Tomasz Grześkowiak, Removal of Bisphenol A and Its Potential Substitutes by Biodegradation, Appl Biochem Biotechnol. 191 (3) (2020) 1100–1110, https://doi.org/10.1007/s12010-020-03247-4.
[15] A. Garg, T. Singhania, A. Singh, S. Sharma, S. Rani, A. Neogy, S.R. Yadav, V. K. Sangal, N. Garg, Photocatalytic Degradation of Bisphenol-A using N, Co Codoped TiO 2 Catalyst under Solar Light, Sci. Rep. 9 (2019) 765, https://doi.org/10.1038/s41598-018-38358-w.
[16] A. Bhatnagar, I. Anastopoulos, Adsorptive removal of bisphenol A (BPA) from aqueous solution: A review, Chemosphere 168 (2017) 885–902, https://doi.org/10.1016/j.chemosphere.2016.10.121.
[17] Anna Kubiak, Marcin Maćkiewicz, Magdalena Biesaga, Marcin Karbarz, Highly efficient removal of bisphenols from aqueous solution using environmental-sensitive microgel, J. Environ. Chem. Eng. 9 (1) (2021) 104947, https://doi.org/10.1016/j.jece:2020.104947.
[18] L. Xu, X. Qian, J. Wu, Electrochemical degradation of aqueous bisphenol A using Ti/SnO2-Sb/Ce-PbO2 anode, IOP Conf. Ser.: Earth Environ. Sci. 508 (2020), 012130, https://doi.org/10.1088/1755-1315/508/1/012130.
[19] Chun-wei Yang, Degradation of bisphenol A using electrochemical assistant Fe(II)-activated peroxydisulfate process, Water Sci. Eng. 8 (2) (2015) 139–144, https://doi.org/10.1016/j.wse.2015.04.002.
[20] Yu-hong Cui, Xiao-yan Li, Guohua Chen, Electrochemical degradation of bisphenol A on different anodes, Water Res. 43 (7) (2009) 1968–1976, https://doi.org/10.1016/j.watres.2009.01.026.
[21] Hideki Kuramitz, Minako Matsushita, Shunitz Tanaka, Electrochemical removal of bisphenol A based on the anodic polymerization using a column type carbon fiber electrode, Water Res. 38 (9) (2004) 2331–2338, https://doi.org/10.1016/j.watres.2004.02.023.
[22] G. Ashraf, M. Asif, A. Aziz, Z. Wang, X. Qiu, Q. Huang, F. Xiao, H. Liu, Nanocomposites consisting of copper and copper oxide incorporated into MoS4 nanostructures for sensitive voltammetric determination of bisphenol A, Microchim Acta. 186 (2019) 337, https://doi.org/10.1007/s00604-019-3406-9.
[23] M. Jędrzejewska-Szczerska, D. Majchrowicz, M. Hirsch, P. Struk, R. Bogdanowicz, M. Bechelany, V.V. Tuchin, Chapter 14 - Nanolayers in Fiber-Optic Biosensing, in: D.P. Nikolelis, G.-.P. Nikoleli (Eds.), Nanotechnology and Biosensors, Elsevier, 2018, pp. 395–426, https://doi.org/10.1016/B978-0-12-813855-7.00014-3.
[24] Y. Bao, M.S. Hoehler, C.M. Smith, M. Bundy, G. Chen, Measuring Three-Dimensional Temperature Distributions in Steel-Concrete Composite Slabs Subjected to Fire Using Distributed Fiber Optic Sensors, Sensors. 20 (2020) 5518, https://doi.org/10.3390/s20195518.
[25] P. Listewnik, M. Bechelany, M. Szczerska, Microsphere-based Fiber-Optic Sensors with ALD ZnO Coatings for Refractive Index and Temperature Measurements (2020), https://doi.org/10.3390/ecsa-7-08222.
[26] Fei Lu, Ruishu Wright, Ping Lu, Patricia C. Cvetic, Paul R. Ohodnicki, Distributed fiber optic pH sensors using sol-gel silica based sensitive materials, Sens. Actuators, B 340 (2021) 129853, https://doi.org/10.1016/j.snb.2021.129853.
[27] Yang Cui, Yi Jiang, Tianmu Liu, Jie Hu, Lan Jiang, A Dual-Cavity Fabry-Perot Interferometric Fiber-Optic Sensor for the Simultaneous Measurement of High-Temperature and High-Gas-Pressure, IEEE Access 8 (2020) 80582–80587, https://doi.org/10.1109/Access.628763910.1109/ACCESS.2020.2991551.
[28] Yong Zheng, Jie Yu, Zheng-Wei Zhu, Bin Zeng, Chao Yang, Design, sensing principle and testing of a novel fiber optic displacement sensor based on linear macro-bending loss, Optik. 242 (2021) 167194, https://doi.org/10.1016/j.ijleo.2021.167194.
[29] Y. Bao, Y. Huang, M.S. Hoehler, G. Chen, Review of Fiber Optic Sensors for Structural Fire Engineering, Sensors. 19 (2019) 877, https://doi.org/10.3390/s19040877.
[30] J. Shin, Z. Liu, W. Bai, Y. Liu, Y. Yan, Y. Xue, I. Kandela, M. Pezhouh, M. R. MacEwan, Y. Huang, W.Z. Ray, W. Zhou, J.A. Rogers, Bioresorbable optical sensor systems for monitoring of intracranial pressure and temperature, Science, Advances. 5 (2019) eaaw1899, https://doi.org/10.1126/sciadv.aaw1899.
[31] Marzena Hirsch, Paulina Listewnik, Przemysław Struk, Matthieu Weber, Mikhael Bechelany, Małgorzata Szczerska, ZnO coated fiber optic microsphere sensor for the enhanced refractive index sensing, Sens. Actuators, A 298 (2019) 111594, https://doi.org/10.1016/j.sna.2019.111594.
[32] Ümit Özgür, Daniel Hofstetter, Hadis Morkoç, ZnO Devices and Applications: A Review of Current Status and Future Prospects, Proc. IEEE 98 (7) (2010) 1255–1268, https://doi.org/10.1109/JPROC.2010.2044550.
[33] D.K. Sharma, S. Shukla, K.K. Sharma, V. Kumar, A review on ZnO: Fundamental properties and applications, Mater. Today:. Proc. (2020), https://doi.org/10.1016/j.matpr.2020.10.238.
[34] J. Theerthagiri, Sunitha Salla, R.A. Senthil, P. Nithyadharseni, A. Madankumar, Prabhakarn Arunachalam, T. Maiyalagan, Hyun-Seok Kim, A review on ZnO nanostructured materials: energy, environmental and biological applications, Nanotechnology. 30 (39) (2019) 392001, https://doi.org/10.1088/1361-6528/ab268a.
[35] M. Kosowska, P. Jakóbczyk, M. Rycewicz, A. Vitkin, M. Szczerska, Low-coherence photonic method of electrochemical processes monitoring, Sci. Rep. 11 (2021) 12600, https://doi.org/10.1038/s41598-021-91883-z.
[36] Roman Viter, Adib Abou Chaaya, Igor Iatsunskyi, Grzegorz Nowaczyk, Kristaps Kovalevskis, Donats Erts, Philippe Miele, Valentyn Smyntyna, Mikhael Bechelany, Tuning of ZnO 1D nanostructures by atomic layer deposition and electrospinning for optical gas sensor applications, Nanotechnology. 26 (10) (2015) 105501, https://doi.org/10.1088/0957-4484/26/10/105501.
[37] Jamil Elias, Mikhael Bechelany, Ivo Utke, Rolf Erni, Davood Hosseini, Johann Michler, Laetitia Philippe, Urchin-inspired zinc oxide as building blocks for nanostructured solar cells, Nano Energy 1 (5) (2012) 696–705, https://doi.org/10.1016/j.nanoen.2012.07.002.
[38] G.F. Pereira, R.C. Rocha-Filho, N. Bocchi, S.R. Biaggio, Electrochemical degradation of bisphenol A using a flow reactor with a boron-doped diamond anode, Chem. Eng. J. 198–199 (2012) 282–288, https://doi.org/10.1016/j.cej.2012.05.057.
[39] M. Rajab, C. Heim, T. Letzel, J.E. Drewes, B. Helmreich, Oxidation of bisphenol A by a boron-doped diamond electrode in different water matrices: transformation products and inorganic by-products, Int. J. Environ. Sci. Technol. 13 (2016) 2539–2548. https://doi.org/10.1007/s13762-016-1087-z.
[40] M. Murugananthan, S. Yoshihara, T. Rakuma, T. Shirakashi, Mineralization of bisphenol A (BPA) by anodic oxidation with boron-doped diamond (BDD) electrode, J. Hazard. Mater. 154 (1-3) (2008) 213–220, https://doi.org/10.1016/j.jhazmat.2007.10.011.
[41] Noémie Elgrishi, Kelley J. Rountree, Brian D. McCarthy, Eric S. Rountree, Thomas T. Eisenhart, Jillian L. Dempsey, A Practical Beginner's Guide to Cyclic Voltammetry, J. Chem. Educ. 95 (2) (2018) 197–206, https://doi.org/10.1021/acs.jchemed.7b00361.
[42] A. Yan, X. Wu, H. Liu, Predicting visibility of interference fringes in X-ray grating interferometry, Opt. Express, OE. 24 (2016) 15927–15939, https://doi.org/10.1364/OE.24.015927.